The fragile-to-strong dynamical crossover and the system viscoelasticity in attractive glass forming colloids

Citation: Mallamace, F., C. Corsaro, D. Mallamace, and S.-H. Chen. "The Fragile-to-Strong Dynamical Crossover and the System Viscoelasticity in Attractive Glass Forming Colloids." Colloid and Polymer Science 293:11 (August 15, 2015), pp.3337–3349.

As Published: http://dx.doi.org/10.1007/s00396-015-3713-6

Publisher: Springer Berlin Heidelberg

Persistent URL: http://hdl.handle.net/1721.1/103372

Version: Author's final manuscript: final author's manuscript post peer review, without publisher's formatting or copy editing

Colloid and Polymer Science manuscript No.
(will be inserted by the editor)

The fragile-to-strong dynamical crossover and the system viscoelasticity in attractive glass forming colloids*

F. Mallamace · C. Corsaro · D. Mallamace · S.-H. Chen

Received: date / Accepted: date

Abstract The dynamical arrest phenomena of an adhesive hard-sphere (AHS) colloid, L64-D_2O system has been studied by using calorimetry and the complex shear modulus. This system is characterized by a rich temperature (T) and volume fraction (ϕ) phase diagram with a percolation line (PT). According to **the** mode-coupling theory (MCT), a cusp-like singularity and two glassy phases, one attractive (AG) and one repulsive (RG), are supposed to coexist in the phase diagram. The MCT scaling laws used to study the shear viscosity with ϕ and T as control parameters propose the existence of fragile-to-strong dynamic crossover (FSDC) **analogous to** that observed in molecular supercooled liquid glass formers. The measured critical values of the control parameters, coincident with the PT line, where the clustering process generates the AG phase, define the FSDC locus. **This is in agreement** with the extended mode-coupling theory that takes into account both cage and inter-cluster hopping effects. **In this work we** demonstrate, by considering the frequency dependence of the complex moduli**, that there is the onset of a system viscoelasticity as an effect of the clustering accompanying the FSDC.** We will show as the measured frequency-dependent complex moduli satisfy the scaling relations predicted by the scalar elasticity percolation theory and well account for the system evolution toward the glass transition process.

Keywords dynamical arrest · adhesive hard-sphere · dynamical crossover

*This paper is dedicated to Professor Heinz Hoffmann on the occasion of his 80^{th} birthday in celebration of his long-time friendship with both of us (Professors Sow-Hsin Chen and Francesco Mallamace). For SHC, he has cherished the happy and productive memory during his stay at the University of Bayreuth as a Humboldt US Senior Scientist Awardee in 1988 and then the revisit again in 1995. During those two periods, he worked closely with Professors Heinz Hoffmann and Jürgen Kalus, and has established invaluable long-lasting friendship as well as constant scientific dialogue with them throughout the years in the last quarter century. FM thanks Heinz and Claudia for the sincere friendship born in the organization of a memorable meeting of the European Colloid and Interphase Science (ECIS) held in Copanello (Italy) on September 1990. We look forward to many more years of productive scientific discussions with Prof. Hoffmann!

F. Mallamace · S.-H. Chen
Department of Nuclear Science and Engineering, Massachusetts Institute of Technology, Cambridge MA 02139, USA
E-mail: francesco.mallamace@unime.com
E-mail: sowhsin@mit.edu

F. Mallamace · C. Corsaro
CNR-IPCF Messina, Viale F. Stagno D'Alcontres 37, 98166 Messina
Dipartimento di Fisica e Scienze della Terra, University of Messina, Viale F. Stagno D'Alcontres 31, 98166 Messina

D. Mallamace
Dipartimento SASTAS, University of Messina, Viale F. Stagno D'Alcontres 31, 98166 Messina

1 Introduction

The dynamical arrest (or glass transition) process toward which supercooled liquids evolve in their glassy phase **poses** for science of slow dynamics an intriguing and open question [1]. Such an argument hence constitutes nowadays a challenging research subject in many different areas **such as** chemistry, physics and biology. To treat the subject, theoretical and statistical physics propose different approaches and models ranging from local dynamical heterogeneities to the energy landscape description of transition states and activated processes [2–4].

The basic idea of the energy landscape model, largely used to study supercooled fluids, is that in complex materials and systems there are many thermodynamical states where the free energy surface has several local minima separated by large barriers. In other words, the system evolves, in exploring its space of phases, with a trajectory that is an alternating sequence of local energy minima (basins) and saddle points (transition states), associated with the positions of all the system particles. A trajectory thus specifies the path of the system as it evolves by moving on its potential energy landscape. **This** seems to explain not only the evolution of supercooled liquids into their amorphous phase but also aging phenomena as far as polymers evolution from the sol to the gel phase [5, 6] or the self-organization of biosystems starting from basic molecules [7, 8]. **Indeed**, the energy landscape model seems to be the key to represent the pathways with which molecular systems evolve to the mesoscale structures acquiring specific functional behaviors [5]. Within this framework, the short-time dynamics **of supercooled** liquids is described as **an** intrabasin motion and the long-time slow dynamics as **an** interbasin motion.

As it is well known, the vitrification process of a liquid is accompanied by a dramatic dynamic slowing down that changes the system properties. **Hence we analyze the system transport quantities (e.g., viscosity η, self-diffusion constant D_s, and relaxation times τ) as a function of the thermodynamic variables (such as temperature T and concentration C) to clarify its microscopic origin** [9]. **In the glass-transition literature this approach has received much attention experimentally, numerically and theoretically. The usual methodology considers** to explore the T-dependence of these coefficients by supercooling liquids into the metastable state below the melting temperature T_M until they either crystallize or vitrify. **However, also** the concentration (or the volume fraction ϕ) **has often been** used as the control parameter [10–15], e.g., in complex fluids (supramolecular systems, polymers, colloids, and granular materials). For such a reason colloids have represented a proper system to clarify many aspects of the glass transition.

The parametrization of transport coefficients inside the supercooled regime has been extensively treated by means of the Vogel-Fulcher-Tammann (VFT or super Arrhenius - SA) empirical form: $\eta = \eta_0 \exp\left(BT_0/(T-T_0)\right)$, indicating $T_0 \ll T_g$ as a finite diverging temperature (associated with the Kauzmann temperature T_K [3, 16]). Supercooled liquids have been classified into two separate categories, "fragile" or "strong" glass formers just by using this form [17]: whereas "strong" liquids exhibit pure Arrhenius (AE) $T-$dependence : $\ln(\eta/\eta_0) = E/k_BT$, **"fragile" liquids show** a VFT behavior. For these reasons in the past years the VFT has been treated as a "universal" feature [18]. **However, recent studies** suggest that the validity of this form must be reconsidered because different experimental and theoretical reasoning show that it lacks physical meaning [6,19–21]. For example, it has been pointed out that $B = D_T T_0$ does not in fact yield the Arrhenius form for $T_0 = 0$ [22].

On these bases, various recent studies [6,21,23] **propose to consider at least two dynamic regimes in order to study the supercooled liquid dynamics in a broader range of temperature.** In fact, an intriguing and important phenomenon **manifests** at a temperature between T_g and T_M inside the supercooled phase [24]: the so called fragile-to-strong dynamic crossover (FSDC) occurring at T_B ($T_g < T_B < T_M$). Lately T_B has been also recognized as a milestone on the way with which systems approach the dynamical arrest since a lot of exceptional processes disclose their properties there.

The most significant seem to be: (a) the splitting of the high T relaxation into the primary (α) and the Johari-Goldstein β_{JG} relaxation times (also named secondary or β_{slow}) [25]. (b) The violation of the Stokes-Einstein (SE) relation with a fractional behavior and the decoupling between the translational and the rotational diffusion (for $T < T_B$). In the high T-regime, as evidenced by the SE, the translational diffusion, D_s, tracks the inverse of the shear viscosity (η^{-1}) whereas for $T < T_B$, D_s declines far less rapidly by decreasing T as $D_s \sim \eta^{-\xi}$, with $\xi \simeq 0.75$; instead D_{Rot} (or the rotational correlation time) remains proportional to the inverse of the shear viscosity down to T_g [26, 27]. (c) It is believed that the FSDC is closely related to the appearing of dynamical heterogeneities (DH), although some pure Arrhenius systems show them [28]. DH **refer** to the presence of transient spatially separated regions with vastly different relaxation times [26, 27, 29]. (d) Usually a fragile to less fragile (or strong) transformation occurs when passing T_B [6]. (e) The hopping extended mode coupling theory (EMCT) identifies T_B with the MCT critical temperature T_c [9, 30–32]. Regarding this latter point we stress that MCT has been used in the past to determine the temperature at which fragile supercooled liquids undergo dynamic changes below T_M [21, 24]. Exploration of all these phenomena can help to stress more the importance of the dynamical crossover [5, 23] and its universality [6].

Starting from **the** temperature-derivative analysis of dielectric relaxation data [33]**,** different approaches have been proposed for estimating T_B such **as the** Adam–Gibbs theory [5,21], the apparent enthalpy space

[23] and also the ideal MCT [6,32]. The FSDC concept can be considered of true interest not only for the way in which a system arrests its dynamics but also for the new science frontiers towards the meso-scales. In this frame, recently has been explicitly considered the idea that around T_B there is the onset of a viscoelastic behavior associated with a clustering process of the system molecules and the resulting energy landscape [5]. Another reason this latter for which T_B appears to be of central interest in material science.

Motivated by this, we studied here the frequency dependence of the shear viscosity and the corresponding moduli of a copolymer micellar system with a short-range attraction due to an effective intermicellar interaction [34]. This adhesive hard-sphere (AHS) colloidal system is an aqueous solution of a nonionic, three-block copolymer made of polyethylene and polypropylene oxides (Pluronic L64). **This polymer is** a T-dependent surfactant forming monodisperse spherical micelles in a wide $T-\phi$ range. As proposed by many experiments [14,34–39] this AHS colloid presents a very rich phase diagram due to the intermicellar interaction (Figure 1a). Besides of an inverted bimodal line with a lower consolute critical point**,** the colloid has a $T-\phi$ dependent percolation line (PT) and, as predicted by the MCT, a rich glass behavior (cusp bifurcation or singularity) [13], due to a hard core and an additional short-range attractive interaction (i.e. AHS). In addition to particle packing ϕ (used for HS colloids to describe the fold singularity), T serves as a second external control parameter. The system is thus characterized by a reentrant liquid-to-glass transition with two liquid-glass transition lines [13]. At high T and sufficiently high ϕ, the system evolves into the well-known "repulsive" glassy state (RG). At relatively low T, however, an "attractive glass" **(AG) forms** and the particle motion is hindered by clustering.

This allowed to divide spherical colloidal systems into two main categories, (i) a one-length-scale hard-sphere system in which glass formation is dictated by the cage effect, and (ii) a two-length-scale AHS with a second glass-forming mechanism: a clustering process caused by interparticle attraction. We stress here that HS colloids have been successful used to study the MCT validity, just by considering concentration as the control parameter [10–12].

In this paper, written on the occasion of the celebration of Heinz Hoffmann, who has made significant contributions to colloidal science, we discuss in terms of the Mode-Coupling Theory the implication of the fragile-to-strong dynamical crossover and the viscoelasticity in a supercooled glass forming system by using as a model system just a colloidal suspension made by an adhesive hard-sphere (AHS) **of** Pluronic L64 and heavy water. In particular we report data coming out from calorimetric and viscoelastic measurements.

2 Current state-of-the-art

Colloidal systems in general share a unique feature, their interparticle interaction potential is usually short ranged, i.e., small if compared to the particle size. They also **exhibit rich** phase behaviors that are in some way manifestations of this potential: the existence of a liquid–liquid phase separation (a bimodal line with the associated critical point), a percolation transition line and a structural arrest state (glassy state) that is the most interesting one.

From a kinetic viewpoint, the dynamics of a supercooled liquid will slow down dramatically. Instead of **crystallizing (the true equilibrium ground state)**, it undergoes a so-called structural arrest transition or kinetic glass transition (KGT) and turns into an amorphous glass, in which the local particle configuration deviates from **that of** the thermodynamical equilibrium state and its motion is hindered by the presence of a long lived cage formed by its neighbors.

The KGT in supercooled liquids has been extensively studied and, for a class of systems in which the potential of interaction among the particles can be modelled as a hard sphere (HS) interaction, many valuable insights have resulted from the ideal MCT calculations [9–12]. In this frame colloids have constituted a model system. The major theoretical predictions are summarized as follows: at low ϕ the behavior of the HS system is fluid-like; as ϕ increases, the density–density correlation function (ISF) of the particles exhibits a two-stage relaxation process: an initial β decay (the rattling of a typical particle confined within a transient cage formed by its neighbors) followed by a slow decay, α, resulting from the cage relaxation and the escape of the trapped particle by rearranging its nearest neighbor configuration. In this latter process the particle diffusion will be coupled to the structural relaxations and the system dynamics will be much slower when its volume fraction is near a certain "critical" value, beyond which the system will be 'arrested' in an amorphous state.

The experimental results showed that the application of the KGT to colloidal systems is highly successful. If a spherical colloidal system is treated as a HS fluid, the connection can be seen explicitly. For a spherical colloidal system, for $\phi < 0.49$ only the fluid phase is found, whereas in the range $0.49 < \phi < 0.55$ the equilibrium state is the two-phase coexistence of a fluid and a crystal (FCC). By manipulating the colloids**, just to avoid crystallization (low polydis-**

persity), the KGT was observed [11] at a critical volume fraction ϕ_c (predicted at 0.516). These findings have been **further** confirmed by involving several model hard sphere systems [12,40]. However, some dynamical anomalies, which cannot be interpreted in terms of the HS potential alone, have been also observed [41] and suggest a more care modelling of the interparticle potential for a more complete KGT picture. In fact, a slight modification of the hard sphere interaction potential has been attracting a great deal of attention. Further MCT calculations (see e.g., ref [41]) showed that if a system is characterized by a hard core plus an additional short range attractive interaction, for example by an AHS, a different structural arrest scenario emerges. Theoretically the phase behavior of the AHS is characterized by an effective temperature $T^* = k_BT/u$, the volume fraction of the particles ϕ and the fractional attractive well width $\Theta = \Delta/R$, where $-u$ is the depth of the attractive square well, Δ the width of the well and R the diameter of the particle. Hence, for a given Θ, in addition to ϕ, a second external control parameter, the effective temperature T^*, was introduced into the description of the phase behavior of the system and the KGT can take place either by increasing ϕ or by changing T^*.

Figure 1b **reports** part of the predicted phase diagram based on the AHS with $\Theta = 0.03$. Starting from the re-entrant (glass-to-liquid-to-glass) transition**, the main characteristics of the AHS colloids are evidenced by varying** T^*. At high T^* and at sufficiently high ϕ, the system evolves into the well-known glassy state **(the RG glass)** as a result of the cage effect **that is** a manifestation of the excluded volume due to the existence of the hard core. **At relatively low T^* instead, an 'attractive glass - AG', in which the motion of the typical particle is constrained by the clustering with neighboring particles, can form.** These MCT calculations hence show that T^* and ϕ are the two system control parameters allowing a transition between these two distinct forms of glass. Thus, there is a branch of the KGT line across which transitions between the attractive glass and the repulsive glass are predicted. Must be stressed the new role, if compared with HS systems, of the clustering process between colloidal particles characterizing the AHS materials. Finally, a special feature is the occurrence of an A_3 singularity at which the glass-to-glass transition line terminates . MCT suggests that the long time dynamics of the two distinct structurally arrested states become identical at and beyond this point (the star in Figure 1b).

The symbols in Figure 1b represent the effective temperature T^* determined by fitting the experimental Small Angle Neutron Scattering (SANS) data taken in the liquid state of Pluronic L64 and heavy water here studied [43]. However, for a given value of the depth of the attractive square well, a T increase (for $\phi > 0.47$) represents for the AHS system the possibility of a transition to an AG dominated by a clustering process. The same process **characterizes** the percolation of these colloidal suspensions: the PT line indicated in Figure 1.

Several experiments have confirmed some of these theoretical predictions for AHS, such as the re-entrant glass-to-liquid-to-glass transition phenomenon [15, 44] and the logarithmic relaxation of the glassy dynamics in the liquid **state** in the vicinity of the A_3 singularity [37], which are considered to be the signatures of the glassy dynamics in the two-length-scale system. In addition, experimental investigations focusing on a dense micellar system gave the first report of the glass-to-glass transition line and **of** its associated end point. **The** detailed analysis leads to physical insight **about** the slow dynamics in the two glassy states [14, 36, 43]. The satisfactory agreement between experimental results and MCT calculations for an AHS justifies treating the L64/D_2O micellar systems within the framework of the glass transition.

The glass transition can be viewed as a mathematical singularity in the MCT equation [9]. As previously said, MCT utilizes closed equations of motion—in which equilibrium structure enters as input via the static structure factor $S(q)$—for the normalized density-fluctuation correlation functions $F(q,t)$ at wave-vector q (or the corresponding susceptivity spectra $\chi''(\omega)$ as a function of frequency ω). **For a system with a given interaction potential, MCT predicts that on varying an external control parameter, such as ϕ or T, up to a certain critical value (ϕ_c or T_c), the dynamics of the system will freeze and its associated relaxation time will diverge.**

The ideal MCT explains the critical value of the control parameter as a singularity that results in a bifurcation phenomenon, and the observables are characterized by two different behaviors above and below T_c (or ϕ_c). Above T_c the correlation functions decay to zero according to precise scaling laws (supporting the case for the arrest's universality). Below T_c the interactions of density fluctuations arrest the previous region via cage effects. The task is to clarify whether the dynamic evolution of the system in the region between T_c and T_g is a crossover due to cage effects **or** to some kind of activated transport.

Note that the two MCT temporal contributions are superimposed with the β contribution at the lowest time, whereas in the frequency regime the β-contribution

is located at a frequency above that of the α-peak ($\omega_\alpha = 1/\tau_\alpha$). Near T_c the α-relaxation, which governs the macroscopic time dynamics on the fluid side characterized by a power law and by anomalies in the Debye-Waller factor, exhibits a stretched exponential form [9]. In contrast, the β-process reveals the crossover approaching with two fractal time-decay behaviors (exhibiting non-universal exponents). Short times produce identical dynamics from both the fluid and glass sides, whereas long times produce correlation functions that can saturate in the glass phase but decay algebraically in the fluid phase.

The ideal MCT crossover temperature can be measured using the two time scales and, in particular, for the α-process by means of a power law form, $\tau_\alpha = \tau_{\alpha 0} \left|(T - T_c)/T_c\right|^{-\gamma}$. This power law form clearly describes the transport data of supercooled fluids in the region $T_M > T > T_c$, and thus in the T-range from the stable liquid phase to inside the supercooled phase. MCT also indicates that the glassy relaxation originates in the fold bifurcation of the long–time limit of the normalized density correlator, that is zero in the liquid phase and positive in the glass (the non-ergodicity parameter or the Debye-Waller factor f_q). More precisely, f_q is discontinuous if the control parameter passes some critical value (e.g., ϕ_c or T_c), exhibiting a singularity as a function of the distance $\epsilon = (T - T_c)/T_c = (\phi - \phi_c)/\phi_c$ for $\epsilon = 0$. The quantity $\sigma = C\epsilon$ is designed by the theory as the separation parameter. The $\beta-$relaxation time scales as $t_\sigma = t_0/|\sigma|^{1/2a}$ $(1/2a > 1.27)$, whereas the primary $(\alpha-)$ according to a different power-law divergence, i.e., $\tau_\alpha = B^{-1/b} t_0 |\sigma|^{-\gamma}$ (the non-universal exponent γ is larger than that of t_σ $(1/2a)$ and is $\gamma = [1/(2a) + 1/(2b)]$). The exponents $0 < a \leq a_{\max} = 0.395$ (the critical one) and $0 < b \leq 1$ are related **to** the system dependent exponent parameter λ $(1/2 \leq \lambda < 1)$ via $\lambda = \Gamma(1-a)^2/\Gamma(1-2a) = \Gamma(1+b)^2/\Gamma(1+2b)$. **Note** that these suggestions have been confirmed for polymers or colloidal solutions with ϕ as control parameter. In particular, light scattering experiments made in hard-sphere colloids for $\phi < \phi_c$, by measuring both the self-diffusion coefficient D_s and τ_α, fully support these suggestions giving $\gamma = 2.7$ [11]. In polystyrene-networked-sphere colloids, however, $\gamma = 3.6$ and $\lambda = 0.88$ [41].

On the contrary of the ideal **one**, the extended MCT is able to describe the behavior of the transport parameters in the region $T_c > T > T_g$ (or $\phi_c > \phi > \phi_g$) by predicting a dynamic crossover in τ_α, and D_s (and also in the system viscosity), as implied by the structure of its equations of motion, occurring just near the critical temperature T_c of the idealized version of the theory. Such a crossover is due to the change in the dynamics from the one determined by the cage effect to that dominated by clustering and hopping processes and can be identified as a FSDC in which the α-relaxation time and the self-diffusion cross over from a SA to an AE behavior [30, 31]. This result, obtained for a Lennard-Jones system, also explains the FSDC observed in transport parameters of a variety of glass-forming fluids. **The** EMCT approach also demonstrates that the Stokes-Einstein relation breaks down in different ways on the fragile and strong sides of the FS crossover. By considering these EMCT findings, the main observations are that [32] $T_c = T_B$ appears to be more relevant than T_g or T_0 to the physics of the dynamic arrest, and the universality shown in the master curves from the scaled description of the Stokes-Einstein and Debye-Stokes-Einstein violations is a "ground-breaking" reality that suggests a new approach to exploring arrested processes.

In this EMCT model, the self-diffusion coefficient can be written as $D_s \approx D^{\rm hop} + D^{\rm id}$, with the dynamic crossover at $T \approx T_c$ from $D \approx D^{\rm id}$ to $D^{\rm hop}$. The ideal contribution $D^{\rm id}$, which vanishes at $T_c/T = 1$, is described as $D^{\rm id} \sim \epsilon^\gamma$ **and** represents the dynamical arrest predicted by the idealized version. We also infer that when $T < T_c$ the self-diffusion coefficient exhibits AE behavior. Therefore, on considering the properties of the AHS colloids it is very easy to relate the hopping to the clustering process dominating the system structure: a micelle belonging to a cluster can "flight" to another one; in other words it can escape from an energy basin to another one. Hence the shear viscosity for $T > T_c$ can be studied by using the MCT power law form, $\eta = \eta_0 \epsilon^{-\gamma}$ for both control parameters.

According to this, **we have recently studied** the viscosity of the AHS colloidal system in a large region of the phase diagram. Our findings are that the critical values of the control parameters coincide with the PT line, and that there is a large intermediate region in the phase diagram between the FSDC line and the glass transition line in which the system dynamics is dominated by the presence of large clusters. We have also demonstrated that it is possible, using the conceptual framework provided by extended mode-coupling theory, to describe the way in which a system approaches the dynamic arrest, taking into account both cage and hopping effects. The obtained results also confirm a larger thermodynamic generality for the FSDC phenomenon, which is usually studied only as a function of the temperature. Figure 2 illustrates such a situation in an Arrhenius plot of the normalized viscosities. More precisely in the main plot of figure 2 the crossover temperature normalized representation is reported, $\eta(T)/\eta(T_c)$ vs. T_c/T, of the L64/D_2O vis-

cosity for $\phi = 0.43, 0.46, 0.488, 0.504$ and 0.552. Two separate behaviors above and below $(T_c/T) = 1$ are clearly evidenced. For $T < T_c$ the fluids have a precise Arrhenius behavior whereas, in the opposite case they follow the MCT power law. In Figure 3 the analogous plot **with** the volume fraction as the control parameters is reported: $\eta(\phi)/\eta(\phi_c)$ vs. ϕ_c/ϕ , for $T = 305, 309, 311, 313, 315$ and $318K$. As it can be observed in both cases there is the evidence of the universal behavior proposed for many supercooled fluids, see e.g., ref. [32].

In both cases the viscosity exhibits an initial steep growth as the control parameters increase reflecting typical gelation behavior; at a certain threshold this increase ceases, then the behavior **changes** and is dominated by cluster deformation and screening **effects**. As ϕ increases further, the **viscosity** exhibits a second step growth until structural arrest is reached. The resulting glass transition can be related to the formation of a spanning cluster made of localized particles connected by bonds. As previously stated, MCT indicates that the presence of bonds is the defining difference between attractive and repulsive glasses. From the data fitting of the SA region (T and ϕ as control parameters) we find that the exponent γ ranges from approximately 2.9 to 3.3 in both cases, i.e., values analogous to those measured in the above mentioned polystyrene-networked-sphere colloid ($\gamma = 3.6$) [41]. In addition, all the calculated T_c values are located just above the system percolation threshold, and the AE region extends from T_c to the dynamic arrest. Finally, the inset of Figure 2 shows in a scaled log-log plot the MCT power law behavior ($\eta = \eta_0 \left|(T - T_c)/T_c\right|^{-\gamma}$) for $\phi = 0.256, 0.43, 0.46, 0.488, 0.504$ and 0.552. The corresponding T_c are reported as large open circles in Figure 1a.

3 Methods

Sample, Sample preparation and experiment. The micellar system that we have studied is a triblock copolymer L64, a member of the Pluronic family made of polyethylene oxide (PEO) and polypropylene oxide (PPO). L64 is $(PEO)_{13}(PPO)_{30}(PEO)_{13}$ with a molecular weight of 2990 *Da*. After a purification [45] by removing hydrophobic impurities, the polymer is dissolved in deuterated water (D_2O). At the **lowest** T, both PEO and PPO are hydrophilic, so L64 chains readily dissolve in water, and the polymers exist as unimers. As the temperature increases there is a decrease in the number of hydrogen bonds between water and polymer molecules, PPO becomes less hydrophilic faster than PEO creating an imbalance of hydrophilicity between the end block and the middle block of the polymer molecule. Consequently the copolymer molecules acquire surfactant properties in the aqueous environment and self-assemble with a micellar formation at a well-defined critical micellar temperature–concentration (CMT–CMC) line. As the temperature increases further, water becomes progressively a poorer solvent for both PPO and PEO chains, and the effective micelle–micelle interaction becomes attractive. Evidence for the increased short range micellar attraction as a function of temperature comes from the existence of a lower consolute critical point at $C = 5.0\ wt\%$ and $T = 330.9\ K$ and a percolation line detected via a jump of the zero-shear viscosity of different orders of magnitude [34]. We have explored the dynamically arrested states and their structure in this micellar system as a function of T and ϕ. All the experiments on this $L64/D_2O$ micellar system here reported have been performed by changing T at fixed ϕ; the samples temperature was controlled **with** an accuracy of $0.2°C$.

The micellar interaction is due to a decreasing in solubility of D_2O solvent molecules in PEO corona as temperature increases above the CMC–CMT line [14, 36,43]. When two micelles touch each other, some D_2O molecules in the corona region are squeezed out and the overlapping between the PEO coronas of two micelles gives rise to the characteristic short range attraction [46]. Two different hydrogen bonds (HB) characterize the system: the HB among D_2O molecules and the HB between D_2O molecules and L64 polymers. The responses of these two HB to the thermal fluctuations are different and the increasing short range attraction can be viewed as the consequence of their interplay as a function of temperature, so that the complex glass behavior (re-entrant and glass-to-glass transitions) can be attributed to the competition of these two hydrogen bonds.

The rheological properties of a viscoelastic system are characterized by the dynamical complex viscosity $\eta^*(\omega)$ and by **the** complex shear $G^*(\omega)$, or the compliance $J^*(\omega) = 1/G^*(\omega)$; $G^*(\omega) = G' + iG'' = i\omega\eta^* = i\omega(\eta' + i\eta'')$; G' and G'' are respectively the loss and storage (or elastic) moduli.

In an oscillatory experiment, **such as** the one here performed, the moduli G' and G'' are obtained from the measurement of the time dependence of the stress, σ as: $\sigma = \gamma(G' \sin\omega t + G'' \cos\omega t)$, where γ is the strain amplitude and $\delta(\omega)$ the phase angle between the stress and strain, measured under the condition that the stress amplitude varies as $\sigma = \sigma_0 \sin(\omega t + \delta)$; hence, $G' = (\sigma_0/\gamma)\cos\delta$, and $G''/G' = \tan\delta$ [47]. We performed the rheological measurements using a strain controlled rheometer, in a cone-plate geometry (Rheostress rs150,

Haake). We have determined the linear viscoelastic moduli as the response of the suspension to very small oscillatory shears which weakly perturb the equilibrium structure. To ensure a system linear response, we have tested our system at the different working T and ϕ, as a function of low applied strain γ; hence we decided to work, in the frequency range $(10^{-2} < \omega(\sec^{-1}) < 10)$ at a deformation of 0.04 where the elastic moduli are γ independent. The rheometer was calibrated at the working viscosities (or elastic moduli) by using different newtonian oils**. Since** the studied transitions (percolation and glass) **are** characterized by changes of many orders of magnitude in the viscoelastic quantities, such calibration procedure is very important in order to obtain reliable data. For these latter measurements, to maintain the system in its amorphous state, samples have been shacked directly into the viscometer by working for some minutes at large strains.

As proposed in a previous work the viscosity measured in the L64/D_2O systems (at the fixed frequency $\omega = 1\,\sec^{-1}$, a condition that ensured a linear response) increases of different orders of magnitude due to the effect of the clustering process associated with the percolation transition [48]. Note also that there is a precise frequency dependence of both the loss and storage moduli, $G'(\omega)$ and $G''(\omega)$, respectively. According to theory [49], near the percolation threshold these moduli exhibit a precise universal scaling behavior with G'' dominant over G': $G' \approx G'' \approx \omega^u$, u being an exponent with an expected value of 0.7 ± 0.1 [34]. A situation this latter accompanied by the condition of the angle δ to be $\omega-$independent ($\delta = u\pi/2$).

The specific heat measure was made by using a temperature modulated scanning calorimeter (a heat-modulated variant of the differential scanning calorimeter) a technique very sensitive to enthalpic changes in the studied system [50]. As it is customary for calorimetric experiments, the system specific heat is measured in thermal cycles (heating and cooling in our case) with a proper thermal rate, that in our case was of $6K/hour$.

Samples were prepared at room temperature by dissolving L64 copolymer in deuterated water. The samples were stored at room temperature some hours (or few days) before measurements for stabilization and to ensure **that** a complete aggregation equilibrium was reached. Pluronic L64 was obtained from BASF and deuterated water (purity 99.9%) from Aldrich.

4 Results and discussion

Figure 4 reports specific heat data, $C_p(J/gK)$ versus T, in the temperature interval $273-348K$, for our AHS system at the volume fraction $\phi = 0.5$ (top side) and $\phi = 0.543$ (bottom side). The heating part of the thermal cycle is represented by closed symbols and the cooling one **by** open symbols, respectively. The first broad maximum, observed in both concentrations at about $285K$ corresponds to the surfactant self-aggregation at the CMC. By increasing the temperature a peak in C_p, that **clearly indicates** the onset of a new thermodynamical phase, can be observed for both the volume fractions. For $\phi = 0.5$ the peak maximum is at about $297K$, whereas for $\phi = 0.543$ it is located at about $288K$; on looking at figure 1a we can see that these two temperatures lie very near the percolation (or the MCT T_c) line, i.e., at the FSDC temperature. **This** seems to confirm the previous reported findings evidenced by the viscosity behavior; but an important result is suggested by the second peak in specific heat of the $\phi = 0.543$ data, observable just near $310K$, where (**see bold cross in** Figure 1a) neutron experiments have **suggested** that the glass-to-glass transition from the AG to RG forms should be located [14, 36, 43]. Hence, also from the specific heat data there is a confirmation of the rich phase diagram of AHS colloids.

As previously stated, now we consider an analysis of the system viscoelasticity in order to define the role and the connections of the FSDC **with** these properties. Like the normalized density-fluctuation correlation functions $F(q,t)$, their corresponding susceptivity spectra $\chi''(\omega)$ (usually measured by means of the depolarized light scattering and the dielectric relaxation techniques) can be used to detail the evolution of the supercooled liquid versus its glass phase in terms of the MCT [9]. **These latter approaches have been used in the years for** many supercooled liquids **such as** o-terphenyl (OTP) [51, 52], glycerol [53] and salol [54]. In particular for these systems **the** susceptivity spectra $\chi''(\omega)$ are characterized by peaks with maxima and minima reflecting the properties of the primary α- relaxation that follow the MCT predictions. More precisely, with decreasing T this peak is shifted to lower frequencies and a distinct minimum appears in the $\chi''(\omega)$ spectra**. Moreover** for $T \longrightarrow T_c$ the position of the minimum ($\omega_{\min}$) is shifted to lower frequencies. However, at T_c the α- peak and the minimum do not disappear (as predicted by the ideal MCT) for the effect of hopping **processes**. Also in this case, as far as for the viscosity (or the other transport parameters), the critical temperature T_c can be deduced from the T-dependence of the $\chi''_{\min}$ (the χ'' value at $\omega_{\min}$) by means of MCT scaling forms: $\chi''_{\min} \sim \varepsilon^{1/2}$ and $\omega_{\min} \sim \varepsilon^{1/(2a)}$. In particular the nearly coincidence between T_c and T_B, evidenced for these latter molecular liquids in terms of the transport quantities, can be also observed by an Ar-

rhenius plot of the measured $\chi''_{\min}$. **Figure 5** represents such a situation for the OTP [51] and the Glycerol [53] data; a FSDC can be observed just near the measured T_c of the ideal MCT, $T_c \simeq 230 \pm 5K$ and $275 \pm 5K$, respectively. However, must be stressed that such a $\omega_{\min}$ shift can cover, by decreasing T, many orders of magnitude and in some systems cannot be experimentally resolved.

As evidenced by proper studies, e.g. in glycerol [55], for temperatures inside the glass region i.e., from near $T_g \simeq 190K$, to $\sim 125K$, there are similarities in the frequency dependence of the shear moduli and the susceptivity. In particular, the glycerol shear response, studied using a rheometer working in a plate-plate geometry in terms of the complex compliance $J^*(\omega)$ in a experimental window of $10^6 - 10^{10}$ Pa and of $10^{-3} < \omega(rad\,\mathrm{sec}^{-1}) < 100$, has evidenced a marked viscoelasticity characterized by well defined maxima in $J''(\omega)$. Here instead, we consider for our L64/D_2O AHS system a measure of the complex moduli from the liquid phase to the glassy region (more precisely the AG) in order to give evidence of the connections between the FSDC and the onset of the system viscoelasticity. For that we report at a fixed temperature the evolution of $G''(\omega)$ at different volume fractions, and where possible, we analyze the obtained data by using the ideal MCT as made for the susceptivity spectra $\chi''(\omega)$ of supercooled molecular liquids.

Figure 6 illustrates the real and imaginary part of the shear moduli for the temperatures 295 and $301K$; G' and G'' corresponding to the $0.43 < \phi < 0.53$ interval are reported as a function of the frequency ω. As it can be observed, in both cases the rheological behavior of the system changes on going from the supercooled liquid state to well inside the AG phase on crossing the PT line that according to our previous discussion represents the clustering process. On the basis of the previous discussion, the observed viscoelasticity evolution well represents the system changes, by crossing the FSDC, from one side described by the ideal MCT to another one for which the transport properties and the susceptivities obey to the extended version of the theory. The spectra reported in figure 6 are essentially the same for the two temperatures; the only difference is that in the spectra of $T = 295K$ a concentration corresponding to the system in the liquid phase ($\phi = 0.45$) is also reported.

On looking **to the** $295K$ **data**, we can observe that the moduli behaviors are completely different going from the liquid state ($\phi = 0.45$) to the AG glass ($\phi = 0.53$). G'' is dominant over G' and both moduli increase with frequency showing the behavior observable in Newtonian fluids. Near the percolation both moduli evidence the scaling behavior as due to the clustering process [49] (for $T = 295K$ the region of this scaling is around $\phi = 0.49$, whereas for $301K$ $\phi = 0.43$). This latter behavior, also shown in the loss angle δ that becomes $\omega-$independent, signals the onset of a marked viscoelasticity. In fact, for the **largest** ϕ, on approaching the glass transition, there is a dramatic change in the shear moduli frequency behavior: G'' shows a minimum at a certain $\omega_{\min}$ and G' a flex point near this minimum in the corresponding loss modulus. In this ϕ region, G' dominates over G'' at the largest frequencies and develops a sort of plateau where it varies very slowly with ω. In the percolation region the measured values of the exponent u and of the loss angle δ are $u \sim 0.68$ the $\delta \sim 1.15$, respectively.

The entire behavior of both the moduli, at the percolation and near the glass transition, from the dominance of G' over G'' to the minimum in $G''(\omega)$, **is** related to the clustering process of the AHS system. The colloidal clustering determines, in fact, the temporal (or frequency) dependence of relaxations. At very short times **the relaxation of** density fluctuations reflects the localized motion of individual particles whereas their longer time is essentially due to the clustering effects. At low and moderate concentrations, before the percolation particles can freely diffuse, and after the trapping effect of the clustering becomes dominant and the diffusion is governed by the hopping. **However,** at the same time, changes in the clusters configuration provide a mechanism for energy storage and dissipation contributing to the moduli (i.e., stable clusters mean an elastic structure in which G' dominates). MCT well details such a situation in the time correlators or **in** the corresponding susceptivity, and hence in the shear moduli, suggesting that the $\omega_{\min}$ position and the value of $\chi''_{\min}$ **depend** sensitively on the control parameter according to: $\chi''_{\min} \sim \varepsilon^{1/2}$ and $\omega_{\min} \sim \varepsilon^{1/(2a)}$. A complete test of the latter scaling law can be obtained in a log-log-plot of $\chi''(\omega)$ (or G'' in our data) versus ω, where spectra with different values for the control parameter should merely differ by parallel shift. Such a situation is clearly represented in figure 6 from our data on the loss moduli on approaching the critical volume fraction (or temperature).

Here unfortunately, as far as in supercooled liquids, these extreme values are present for T (or ϕ) above and below their critical value of the ideal MCT, a reason for which we cannot use these latter scaling form. Nevertheless another MCT **approach** can be considered to describe the obtained data. A form successfully used in the analysis of $\chi''(\omega)$ data, measured by depo-

larized light scattering with which a MCT master curve can be found, is:

$$G''(\omega) = G''_{\min}\left[b(\omega/\omega_{\min})^a + a(\omega/\omega_{\min})^{-b}\right]/(a+b) \quad (1)$$

We stress that this interpolation expression is equivalent to the main MCT form for the $\beta-$correlators in the time regime [9]. The full curve in figure 7 is the interpolation form for $\lambda = 0.75$ and $\gamma = 3.1$ (the average value obtained from the viscosity fitting); no volume fraction dependence is found.

As it can be observed the data essentially fall in the obtained master curve. However**, note** that the **low-frequency** flank of the minimum does not follow the same behavior of the concentration near the FSDC. More precisely for $\phi > \phi_c$ the data flatten with **the region of the minimum** that **becomes** broader. The corresponding high-frequency flank instead appears to follow a common envelope. This failure in the scaling for volume fractions above that of the dynamical crossover clearly indicates a change in the dynamics of the system supporting the proposed physical significance of the dynamical crossover for supercooled systems. In conclusion of this second experimental part, on following the system evolution towards the **attractive** glass (AG), we have the confirmation from rheological measurements, that in our adhesive micellar system the clustering process signs the system evolution towards the glass **transition** by means of an high order singularity [13].

5 Concluding remarks

We have presented results coming out from calorimetry, viscosity and complex shear moduli to understand the properties of an AHS colloidal system (an AHS micellar copolymer) that exhibits strong clustering behavior. We have considered a region of its $T-\phi$ phase diagram where **we can be study** some special **features** of the system **that are** driven just **by** the colloidal attraction and hence by the consequent clustering. This region includes the disordered liquid phase, the crossing of the percolation line, the two glassy phases, one attractive (AG) and one repulsive (RG), and finally the glass-to-glass transition. We have done this in terms of the ideal MCT power laws by using as control parameters both T and ϕ obtaining the corresponding critical values T_c and ϕ_c. Above PT the viscosity behavior is purely Arrhenius in both cases. We find that the locus of the measured T_c and ϕ_c in the phase diagram, which defines the dynamical crossover line from a fragile-to-strong glass forming materials, appears to be coincident with the percolation line. A behavior, this latter, typical of molecular supercooled liquids where the FSDC **is only a** function of the temperature **and is** observable very far from the calorimetric glass transition temperature. In an AHS colloidal system the crossover **deals** with AG and hence is a function of the packing fraction ϕ **due to the interparticle attraction and thus to the clustering process**.

With the use of the shear viscosity data, we have observed in this AHS system two, large and distinct phase diagram regions exhibiting contrasting dynamic behaviors: (i) a fragile system exhibiting well-defined super-Arrhenius behavior (described using MCT) that extends from the disordered liquid phase up to the PT line, and (ii) a strong glass-forming system that has higher T and ϕ values and that extends from the PT line (also the locus of the T_c and ϕ_c values) to the glass transition line (figures 2 and 3).

We observe in the strong glass-forming system, as far as in supercooled liquids, a region of anomalous "glassy" dynamics beginning before the actual dynamic arrest (the transition from liquid to amorphous solid) at T_c and ϕ_c (also described using MCT). As mentioned above, MCT explains T_c (and hence also ϕ_c) as a singularity resulting from a bifurcation in the self-trapping problem of density fluctuations. We thus see two different behaviors above and below these singular values, indicating an important crossover between two different dynamics inside the supercooled liquid phase far from the glass transition. Above T_c the physics is clearly defined by the well-known cage effect. But the system dynamics in the region from T_c (or ϕ_c) to the dynamic arrest can be clarified by the clustering properties of the AHS system. We find **that in** this latter case the system evolution is dominated by an activated transport process. The T_c and ϕ_c line thus defines a real crossover in the physical properties of the glass-forming material.

These results are confirmed in the MCT framework, more precisely **by** the EMCT version based on hopping processes. As already mentioned, the pure liquid phase is however described in terms of the classical cage effect. The particle dynamic behavior of the little polydisperse clusters and monomers in this liquid phase is due to a diffusion process in which particles are correlated with each other and do not freely diffuse. If we increase the packing (volume fraction) and the interparticle attractive interactions (temperature) many transport properties change by many orders of magnitude. There is a slowing down, the caging is less effective, and the probability that cage hopping will occur increases. The emerging spanning cluster makes the crossover in the system dynamics possible. Further increases in T and ϕ values impose a new behavior: the only **degree of** freedom left to the particles is hopping.

Due to the colloidal particle interactions the clustering process that starts in the disordered liquid phase becomes more developed near the PT. In the liquid phase there are many monomers and little polydisperse clusters that increase in size on approaching PT. An effect of this interparticle aggregation certainly will result in a mechanism for energy storage and dissipation contributing to **the** frequency dependence of the moduli (i.e. stable clusters mean an elastic structure in which G' dominates). **Hence the onset of a viscoelastic behaviour strongly influences the system dynamics. Finally, we have shown as the measured frequency-dependent complex moduli satisfies the scaling relations predicted by the scalar elasticity percolation theory and well accounts the evolution of the system toward the glass transition process.**

We **conclude that** the observed viscoelasticity can be considered as an additional support on the hypothesis that the FSDC process has **an** universality character.

Acknowledgment. The research at MIT has been supported by DOE Grant No. DE-FG02-90ER45429.

References

1. Debenedetti PG (1996) Metastable Liquids: Concepts and Principles. Princeton Univ. Press, Princeton.
2. Laio A, Parrinello M (2002) Escaping free-energy minima. Proc Natl Acad Sci USA 99:12562–12566. doi:10.1073/pnas.202427399
3. Stillinger FH (1988) Supercooled liquids, glass transitions, and the Kauzmann paradox. J Chem Phys 88:7818–7825. doi:10.1063/1.454295
4. Laughlin RB, Pines D, Schmalian J, Stojkovic BP, Wolynes P (2000) The middle way. Proc Natl Acad Sci USA 97:32–37. doi:10.1073/pnas.97.1.32
5. Yip S, Short MP (2013) Multiscale materials modelling at the mesoscale. Nature Mater 12:774-777. doi:10.1038/nmat3746
6. Mallamace F et al (2010) Transport properties of glass-forming liquids suggest that dynamic crossover temperature is as important as the glass transition temperature. Proc Natl Acad Sci USA 28:22457–22462. doi:10.1073/pnas.1015340107
7. Wolynes PG, Onuchic JN, Thirumalai D (1995) Navigating the folding routes. Science 267:1619–1620. doi:10.1126/science.7886447
8. Karplus M (2011) Behind the folding funnel diagram. Nature Chem Bio 7:401–403. doi:10.1038/nchembio.565
9. Götze W, Sjögren L (1992) Relaxation processes in supercooled liquids. Rep Prog Phys 55:241. doi:10.1088/0034-4885/55/3/001
10. Bengtzelius U, Götze W, Sjölander A (1984) Dynamics of supercooled liquids and the glass transition. J Phys C: Solid State Phys 17:5915. doi:10.1088/0022-3719/17/33/005
11. van Megen W, Pusey P (1991) Dynamic light-scattering study of the glass transition in a colloidal suspension. Phys Rev A 43:5429. doi:10.1103/PhysRevA.43.5429
12. van Megen W, Underwood SM (1994) Glass transition in colloidal hard spheres: Measurement and mode-coupling-theory analysis of the coherent intermediate scattering function. Phys Rev E 49:4206. doi:10.1103/PhysRevE.49.4206; (1993) Glass transition in colloidal hard spheres: Mode-coupling theory analysis. Phys Rev Lett 70:2766. doi:10.1103/PhysRevLett.70.2766 .
13. Fabbian L et al (1999) Ideal glass-glass transitions and logarithmic decay of correlations in a simple system. Phys Rev E 59:R1347. doi:10.1103/PhysRevE.59.R1347 .
14. Chen SH, Chen WR, Mallamace F (2003) The Glass-to-Glass Transition and Its End Point in a Copolymer Micellar System. Science 300:619–622. doi:10.1126/science.1082364 .
15. Pham KN, Egelhaaf SU, Pusey PN, Poon WCK (2003) Glasses in hard spheres with short-range attraction. Phys Rev E 69:011503. doi:10.1103/PhysRevE.69.011503
16. Adams G, Gibbs JH (1965) On the Temperature Dependence of Cooperative Relaxation Properties in Glass-Forming Liquids. J Chem Phys 43:139–146. doi:10.1063/1.1696442
17. Angell CA (1995) Formation of Glasses from Liquids and Biopolymers. Science 267:1924–1935. doi:10.1126/science.267.5206.1924
18. Hansen C et al (1997) Dynamics of glass-forming liquids. III. Comparing the dielectric α- and β-relaxation of 1-propanol and o-terphenyl. J Chem Phys 107:1086-1093. doi:10.1063/1.474456
19. Eckmann JP, Procaccia I (2008) Ergodicity and slowing down in glass-forming systems with soft potentials: No finite-temperature singularities. Phys Rev E 78:011503. doi:0.1103/PhysRevE.78.011503
20. Hecksher T, Nielsen AI, Boye Olsen N, Dyre JC (2008) Little evidence for dynamic divergences in ultraviscous molecular liquids. Nat Phys 4:737–741. doi:10.1038/nphys1033
21. Mauro JC et al (2009) Viscosity of glass-forming liquids. Proc Natl Acad Sci. USA 106:19780–19784. doi:10.1073/pnas.0911705106
22. Johari GP (2006) On Poisson's ratio of glass and liquid vitrification characteristics. Philos Mag 86:1567. doi:10.1080/14786430500398441
23. Martinez-Garcia JC, Martinez-Garcia J, Rzoska SJ, Hulliger J (2012) The new insight into dynamic crossover in glass forming liquids from the apparent enthalpy analysis. J Chem Phys 137:064501. doi:10.1063/1.4739750
24. Taborek P, Kleinman RN, Bishop DJ (1986) Power-law behavior in the viscosity of supercooled liquids. Phys Rev B 34:1835. doi:10.1103/PhysRevB.34.1835
25. Johari GP, Goldstein M (1970) Viscous Liquids and the Glass Transition. II. Secondary Relaxations in Glasses of Rigid Molecules. J Chem Phys 53:2372–2388. doi:10.1063/1.1674335
26. Tarjus G, Kivelson D (1995) Breakdown of the StokesEinstein relation in supercooled liquids. J Chem Phys 103:3071–3073. doi:10.1063/1.470495
27. Ediger MD (2000) Spatially heterogeneous dynamics in supercooled liquids. Ann Rev Phys Chem 51:99–128. doi:10.1146/annurev.physchem.51.1.99
28. Zuriaga MJ, Perez SC, Pardo LC, Tamarit JLl (2012) Dynamic heterogeneity in the glass-like monoclinic phases of CBr_nCl_{4-n}, n = 0,1,2. J Chem Phys 137:054506. doi:10.1063/1.4739531
29. Debenedetti PG, Stillinger FH (2001) Supercooled liquids and the glass transition. Nature 410:259. doi:10.1038/35065704

30. Chong SH (2008) Connections of activated hopping processes with the breakdown of the Stokes-Einstein relation and with aspects of dynamical heterogeneities. Phys Rev E 78:041501. doi:10.1103/PhysRevE.78.041501
31. Chong SH, Chen SH, Mallamace F (2009) A possible scenario for the fragile-to-strong dynamic crossover predicted by the extended mode-coupling theory for glass transition. J Phys: Condens Matter 21:504101. doi:10.1088/0953-8984/21/50/504101
32. Mallamace F, Corsaro C, Stanley HE, Chen SH (2011) The role of the dynamic crossover temperature and the arrest in glass-forming fluids. Eur Phys J E 34:94. doi:10.1140/epje/i2011-11094-7
33. Stickel F, Fisher EW, Richert R (1995) Dynamics of glass-forming liquids. I. Temperature-derivative analysis of dielectric relaxation data. J Chem Phys 102:6251-6257. doi:10.1063/1.469071
34. Lobry L et al (1999) Interaction and percolation in the L64 triblock copolymer micellar system. Phys Rev E 60:7076. doi:10.1103/PhysRevE.60.7076
35. Mallamace F et al (1999) Percolation and viscoelasticity of triblock copolymer micellar solutions. Physica A 266:123. doi:10.1016/S0378-4371(98)00585-8
36. Chen WR, Chen SH, Mallamace F (2002) Small-angle neutron scattering study of the temperature-dependent attractive interaction in dense L64 copolymer micellar solutions and its relation to kinetic glass transition. Phys Rev E 66:021403. doi:10.1103/PhysRevE.66.021403
37. Mallamace F et al (2000) Kinetic Glass Transition in a Micellar System with Short-Range Attractive Interaction. Phys Rev Lett 84:5431. doi:10.1103/PhysRevLett.84.5431
38. Mallamace F et al (2004) (2004) J Phys: Condens Matter 16:S4975. J Phys: Condens Matter 16:S4975. doi:10.1088/0953-8984/16/42/013
39. Mallamace F et al (2006) Complex viscosity behavior and cluster formation in attractive colloidal systems. Phys Rev E 73:020402. doi:10.1103/PhysRevE.73.020402
40. Fuchs F (1995) MCT Results for a simple liquid at the glass transition. Transport Theory Stat Phys 24:855-880. doi:10.1080/00411459508203937
41. Bartsch E, Antonietti M, Schupp W, Sillescu H (1992) Dynamic light scattering study of concentrated microgel solutions as mesoscopic model of the glass transition in quasiatomic fluids. J Chem Phys 97:3950. doi:10.1063/1.462934
42. Dawson K (2002) The glass paradigm for colloidal glasses, gels, and other arrested states driven by attractive interactions. Curr Opin Colloid Interface Sci 7:218. doi:10.1016/S1359-0294(02)00052-3
43. Chen WR et al (2003) Neutron- and light-scattering studies of the liquid-to-glass and glass-to-glass transitions in dense copolymer micellar solutions. Phys Rev E 68:041402. doi:10.1103/PhysRevE.68.041402
44. Eckert T, Bartsch E (2002) Re-entrant Glass Transition in a Colloid-Polymer Mixture with Depletion Attractions. Phys Rev Lett 89:125701. doi:10.1103/PhysRevLett.89.125701
45. Chen SH, Liao C, Fratini E, Baglioni P, Mallamace F (2001) Interaction, critical, percolation and kinetic glass transitions in pluronic L-64 micellar solutions. Colloids Surf A 183–185:95–111.
46. Lemaire B, Bothorel P, Roux D (1983) Micellar Interactions in Water-in-Oil Microemulsions. 1. Calculated Interaction Potential. J Phys Chem 87:1023–1028. doi:10.1021/j100229a021
47. Ferry JD (1980) Viscoelastic Properties of Polymers. Wiley, New York
48. Mallamace F, Corsaro C, Stanley HE, Mallamace D, Chen SH (2013) The dynamical crossover in attractive colloidal systems. J Chem Phys 139:214502. doi:10.1063/1.4833595
49. de Gennes PG (1979) Scaling Concepts in Polymer Physics. Cornell University press, Ithaca
50. Mallamace F et al (2011) Transport properties of supercooled confined water. Riv Nuovo Cim 34:253–388. doi:10.1393/ncr/i2011-10065-4
51. Singh AP et al (1998) Structural relaxation in orthoterphenyl: a schematic mode-coupling-theory model analysis. J Non-Cryst Sol 235-237:66-70. doi:10.1016/S0022-3093(98)00583-3
52. Steffen W, Patkowsi, Gläser H, Meier G, Fisher EW (1994) Depolarized-light-scattering study of orthoterphenyl and comparison with the mode-coupling model. Phys Rev E 49:2992. doi:10.1103/PhysRevE.49.2992
53. Franosch T, Götze W, Mayr MR, Singh AP (1997) Evolution of structural relaxation spectra of glycerol within the gigahertz band. Phys Rev E 55:3183. doi:10.1103/PhysRevE.55.3183
54. Li G, Du M, Sakai A, Cummins HZ (1992) Light-scattering investigation of α and β relaxation near the liquid-glass transition of the molecular glass Salol. Phys Rev A 46:3343. doi:10.1103/PhysRevA.46.3343
55. Schröter K, Donth E (2000) Viscosity and shear response at the dynamic glass transition of glycerol. J Chem Phys 113:9101. doi:10.1063/1.1319616

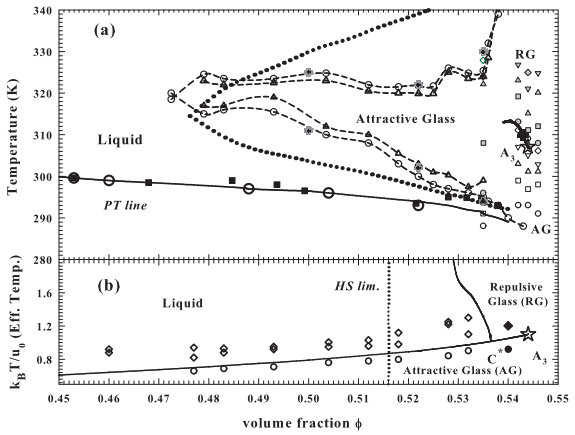

Fig. 1 The L64-D_2O (AHS colloid) phase diagram in the glass region as proposed by light, neutron and viscosity experiments (top side, a) [14, 34, 36, 43]. The system phase diagram in terms of the effective temperature T^*(bottom side, b).

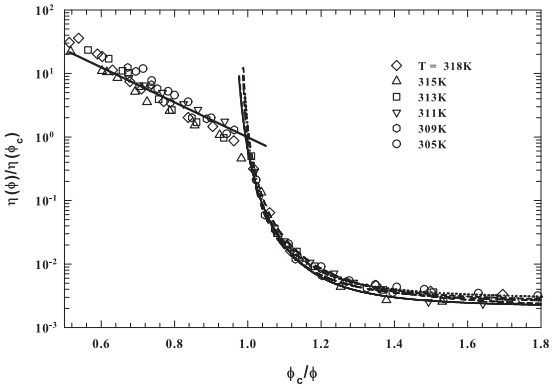

Fig. 3 The normalized viscosity with the volume fraction as control parameter: $\eta(\phi)/\eta(\phi_c)$ vs. ϕ_c/ϕ. **Data** for $T = 305, 309, 311, 313, 315$ and $318K$ **are reported**.

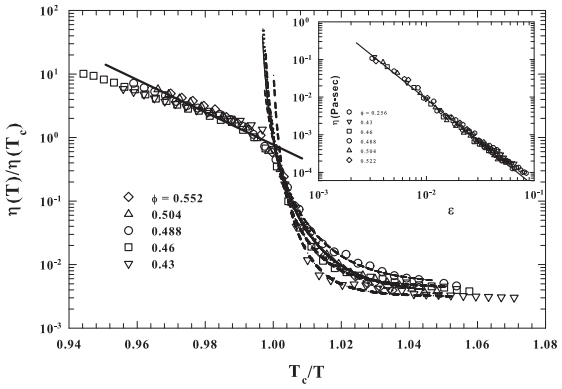

Fig. 2 The temperature normalized representation of the system viscosity, $\eta(T)/\eta(T_c)$ vs. T_c/T. **Data** for $\phi = 0.43, 0.46, 0.488, 0.504$ and 0.552 **are reported**. The inset shows **in** a scaled log-log plot the MCT power law behavior of the viscosity ($\eta = \eta_0 \left|(T - T_c)/T_c\right|^{-\gamma}$) for $\phi = 0.256, 0.43, 0.46, 0.488, 0.504$ and 0.552.

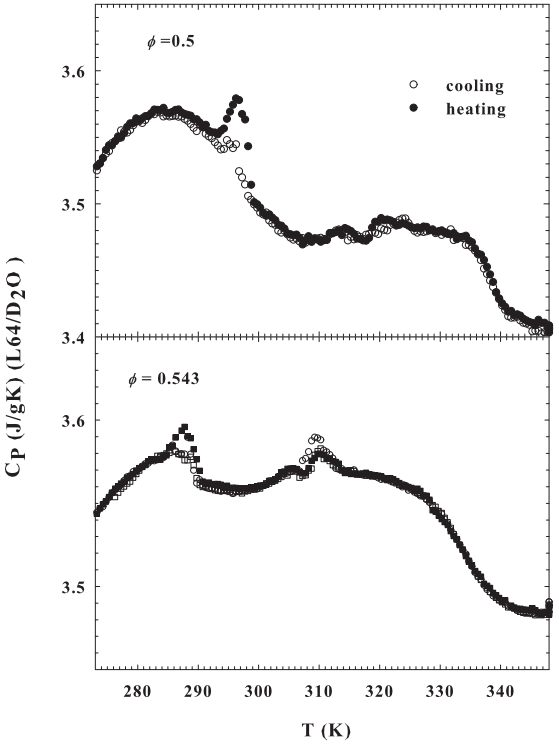

Fig. 4 The specific heat data, $C_p(J/gK)$ versus T, in the temperature interval $273 - 348K$, for our AHS system at the volume fraction $\phi = 0.5$ (top side) and $\phi = 0.543$ (bottom side). The narrow peaks at low T deal with the liquid glass transition. The peak observed at $T = 310$ K for ϕ=0.543 is due to the glass-to-glass transition.

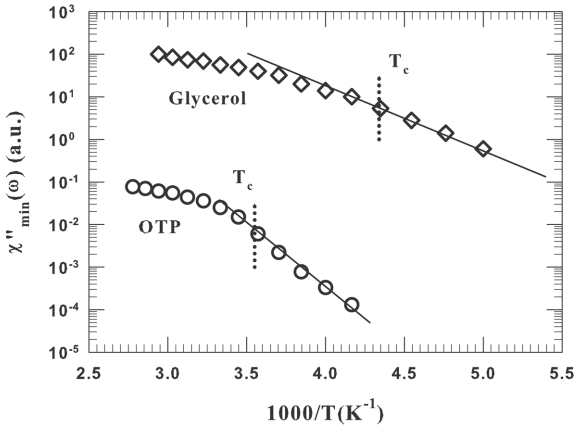

Fig. 5 The evidence of the fragile-to-strong dynamical crossover in OTP and glycerol from an Arrhenius plot of the measured $\chi''_{\rm min}$.

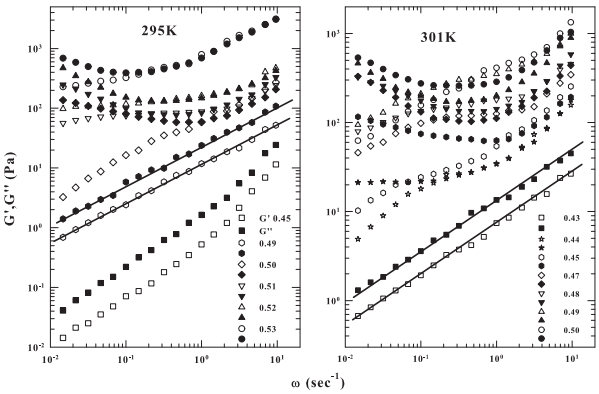

Fig. 6 The real and imaginary part of the shear moduli for the temperatures 295 and $301K$. The G' and G'' measured in the range $0.43 < \phi < 0.53$ are reported as a function of the frequency ω.

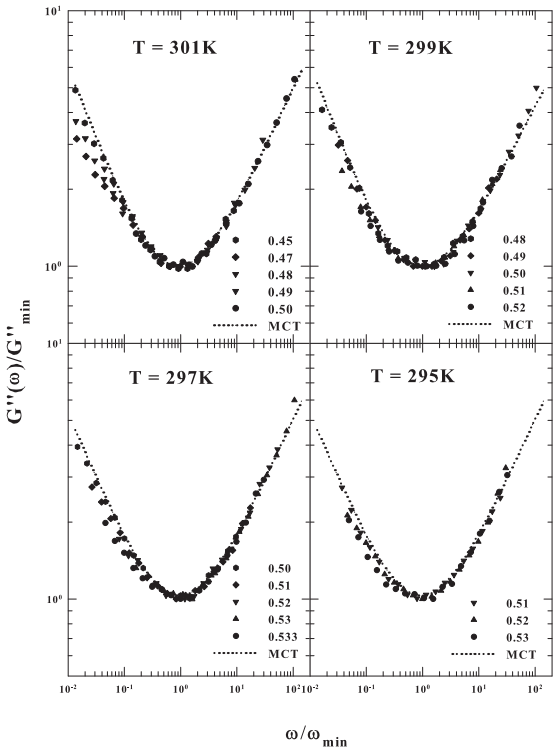

Fig. 7 The rescaled loss moduli $G''(\omega)/G_{\rm min}$ versus $\omega/\omega_{\rm min}$ (data of the Fig. 6). The line is the MCT master spectrum for $\lambda = 0.75$.